# Retrieval of Stratospheric NO$_2$ Vertical Profiles from Ground-Based Zenith-Sky DOAS Measurements: Results for the MANTRA 1998 Field Campaign

Stella M. L. Melo[1*], K. Strong[1], M. R. Bassford[2], K. E. Preston[3],
C. T. McElroy[4], E. V. Rozanov[5] and T. Egorova[5]

[1]*Department of Physics, University of Toronto, Toronto ON*
[2]*Ministry of Defense, London, UK*
[3]*Jacques Whitford Environment Limited, Calgary, Alberta*
[4]*Meteorological Service of Canada, Downsview ON*
[5]*PMOD/WRC and IAC ETHZ, Davos, Switzerland*

ABSTRACT  *The importance of measurements of the vertical distribution of odd nitrogen in studies of ozone chemistry and climate change has long being recognized. In this paper, we use the optimal estimation method developed by Rodgers (1976, 1990) to retrieve NO$_2$ vertical profiles from slant column observations made with a portable ultraviolet (UV)-visible zenith-sky spectrometer operated on the ground during the Middle Atmosphere Nitrogen TRend Assessment (MANTRA) balloon campaign carried out at Vanscoy, Saskatchewan, Canada (52°N, 107°W), from 18 to 25 August 1998. Late summer was chosen for the campaign because the stratospheric zonal wind velocity changes sign at that time. Under such conditions the stratospheric winds are at a minimum, leaving the stratosphere in a dynamically quiescent state and closer to photochemical control (Fahey et al., 2001; Fioletov and Shepherd, 2003). The NO$_2$ profile retrieved from the ground-based observations is compared with the co-located and simultaneous NO$_2$ profile measured by a balloon-borne UV-visible spectrometer during sunrise on 24 August. Good agreement is observed, giving us confidence in the retrieval technique adopted. The retrieved NO$_2$ profiles are also compared with the output of the Model for Evaluating oZONe trends (MEZON) 3D stratospheric chemical transport model. It is observed that, for altitudes below the peak concentration, the model underestimates the NO$_2$ amount, and at the altitude of peak concentration, the model values lie between the values measured from the balloon and those retrieved from the ground-based measurements. Nevertheless, the model reproduces the general shape of the retrieved profiles, including the altitude of the NO$_2$ maximum, for both sunrise and sunset conditions.*

RÉSUMÉ  *[Traduit par la rédaction] L'importance des mesures de la distribution verticale de l'azote radiculaire dans les études de la chimie de l'ozone et du changement climatique est depuis longtemps reconnue. Dans cet article, nous utilisons la méthode d'estimation optimale mise au point par Rodgers (1976, 1990) pour produire des profils verticaux de NO$_2$ à partir d'observations dans une colonne oblique faites à l'aide d'un spectromètre zénithal ultraviolet–visible portatif placé au sol lors de l'Évaluation des tendances de l'azote dans l'atmosphère moyenne (projet MANTRA) qui a eu lieu à Vanscoy (52°N, 107°W), en Saskatchewan, du 18 au 25 août 1998. C'est vers la fin de l'été que la campagne a eu lieu parce que la vitesse du vent stratosphérique zonal change de signe à ce moment. Dans ces conditions, le vent stratosphérique est à son minimum et la stratosphère se trouve dans un état de repos dynamique et plus près d'une régulation photochimique (Fahey et al., 2001; Fioletov and Shepherd, 2003). Nous comparons le profil de NO$_2$ produit à partir des observations faites depuis le sol au profil de NO$_2$ mesuré au même endroit et au même moment par un spectromètre UV-visible emporté par ballon au lever du soleil le 24 août. Les profils s'accordent bien, ce qui nous donne confiance dans la méthode de production adoptée. Nous comparons aussi les profils de NO$_2$ produits du modèle de transport chimique stratosphérique 3D MEZON (Model for Evaluating oZONe trends). On constate que, pour les altitudes en bas de la concentration de pointe, le modèle sous-estime la valeur de NO$_2$, et que, à l'altitude de la concentration de pointe, les valeurs du modèle sont entre les valeurs mesurées du ballon et les valeurs dérivées des mesures au sol.  Toutefois, le modèle reproduit la forme générale des profils produits, y compris l'altitude du maximum de NO$_2$, tant lors du lever que du coucher du soleil.*

## 1 Introduction

Interest in atmospheric nitrogen dioxide (NO$_2$) is largely due to its important role in ozone photochemistry, which is strongly dependent on altitude. Below 25 km, NO$_2$ moderates O$_3$ loss by converting active chlorine and hydrogen species to inactive forms, while between 25 and 40 km, NO$_2$ is involved in a catalytic cycle (Crutzen, 1970) that accounts for almost

---

*Corresponding author's e-mail: stella.melo@space.gc.ca; Current affiliation: Canadian Space Agency, 6767 route de l'Aeroport, Saint-Hubert QC J3Y 8Y9

half of the $O_3$ removed by gas phase reactions (Garcia and Solomon, 1994). The combination of these destruction cycles with those involving odd chlorine and bromine, odd oxygen, and odd hydrogen determines the photochemical balance of stratospheric $O_3$. Therefore, it is important to determine not only the total column but also the altitude distribution of the $NO_2$ concentration.

In this work we apply the optimal estimation method developed by Rodgers (1976, 1990, 2000) to retrieve $NO_2$ vertical profiles from ground-based measurements of $NO_2$ slant column variation with solar zenith angle (SZA) made during the Middle Atmosphere TRend Assessment (MANTRA) 1998 field campaign. The balloon carried a payload containing an ultra-violet (UV)-visible spectrometer that measured the $NO_2$ vertical distribution during sunrise on 24 August, providing a unique opportunity to test the retrieval method adopted here for our ground-based instrument. This comparison is presented and discussed below, and the measurements are compared with the output of the Model for Evaluating oZONe trends (MEZON) 3D stratospheric chemical transport model.

Ground-based instrumentation can provide long-term temporal coverage over a specific location. Because the instrument can receive regular maintenance, its stability can be assured giving a dataset that can be used for satellite comparison. Satellite-borne instruments such as the Optical Spectrograph and InfraRed Imager System (OSIRIS) (on Odin), the Scanning Imaging Absorption SpectroMeter for Atmospheric Chartography (SCIAMACHY), the Michelson Interferometer for Passive Atmospheric Sounding (MIPAS) and the Global Ozone Monitoring by Occultation of Stars (GOMOS) (on Envisat), the Measurement of Aerosol Extinction in the Stratosphere and Troposhere Retrieved by Occultation (MAESTRO) and the Atmospheric Chemistry Experiment (ACE) (on SCISAT-1) all need datasets acquired from different platforms for validation of their $NO_2$ profile measurements. Therefore, the method discussed here is of particular relevance to satellite evaluation because it can be used to provide vertical profiles of $NO_2$ concentration from ground-based zenith-sky measurements that are routinely acquired at mid-latitude observatories or during campaigns.

## 2 Observations

MANTRA 1998 was a balloon campaign to investigate changes in the concentration of nitrogen and chlorine compounds and $O_3$ in the stratosphere. It involved the launch of an 11.6 million cubic feet balloon from Vanscoy, Saskatchewan, Canada (52°N, 107°W, 511.0 m) at 09:25:25 UTC on 24 August 1998. The balloon carried a payload of instruments that measured a variety of stratospheric trace constituents including $O_3$ and $NO_2$. A complete description of the MANTRA 1998 campaign is given by Strong et al. (this issue).

The balloon-borne spectrometer used to measure $NO_2$ is a photodiode array grating spectrometer, based on the SunPhotoSpectrometer (SPS) that has been flown aboard the National Aeronautics and Space Administration's (NASA) ER-2 aircraft as the Composition and Photodissociative Flux Measurement (CPFM) experiment (McAfee et al., 1994; McElroy, 1995). In brief, during the MANTRA campaign, this instrument recorded solar spectra from 375 to 775 nm at 1.7 nm resolution in solar occultation mode for sunrise. The spectral region from 400 to 550 nm was used to recover the apparent column densities of $NO_2$ by using the chi-squared minimization technique. The vertical profile of $NO_2$ was retrieved using the Chahine relaxation method (McKenzie et al., 1991). The errors in the retrieved $NO_2$ mixing ratios are estimated to be ±10% of the retrieved values.

A portable ground-based UV-visible grating spectrometer was used to measure $NO_2$ during the campaign. The instrument, described in detail by Bassford et al. (this issue), is housed in a watertight aluminum box with a top-mounted Plexiglas window (UV-grade) to provide a zenith view of the sky. Zenith-scattered sunlight is focused onto the entrance slit of an imaging spectrometer that disperses the light onto a CCD array detector. The data used here were acquired with a slit width of 50 µm and a diffraction grating ruled at 600 grooves mm$^{-1}$, which produced a full-width half-maximum resolution of 0.90 nm.

Twilight zenith-sky spectra from 320 to 554 nm were recorded daily from 18 to 25 August at solar zenith angles up to approximately 96° during both sunrise and sunset. The integration time was varied throughout the day to compensate for changes in the light levels in order to maximize the total signal and the number of accumulations comprising a spectrum. However, the maximum total accumulation time was restricted to five minutes which, at the launch site during twilight in August, corresponds to a change in SZA of 0.7°.

The spectra were analysed using the well-known differential optical absorption spectroscopy (DOAS) technique (e.g., Brewer et al., 1973; Noxon, 1975; Solomon et al., 1987; Platt, 1994; Otten et al., 1998). In essence, the technique utilizes the fact that scattered sunlight observed at twilight traverses a much longer stratospheric path than that observed at noon. The analysis bandwidth was 405 nm to 450 nm, the region where $O_3$ absorption is reduced. The spectral analysis utilizes absorption cross-sections of $O_3$ (Burrows et al., 1998), $O_2$-dimer (Greenblatt et al., 1990), $H_2O$ (Sarkissian, 1992), and $NO_2$ (Burrows et al., 1998). Raman scattering is believed to cause infilling of the solar Fraunhofer lines in spectra of scattered sunlight. This phenomenon, referred to as the Ring effect (Grainger and Ring, 1962), is taken into account by using a Ring cross-section calculated using the model of Chance and Spurr (1997).

The noon spectrum measured on 25 August (Julian day 237) 1998 was chosen as a common reference spectrum. The slant and vertical $NO_2$ columns derived for each day of the campaign are retrieved and discussed by Bassford et al. (this issue).

As part of the MANTRA campaign, ozonesondes and radiosondes were launched almost daily during the two weeks prior to the balloon launch in order to characterize the local atmosphere (winds, pressure, temperature, $O_3$, and humidity).

The resulting O$_3$ partial pressure and temperature profiles were incorporated into our retrieval process.

## 3 Retrieval technique

A detailed description of the retrieval method adopted here, including a rigorous error analysis and validation studies, is given by Preston (1995), Preston et al. (1997, 1998), and its application to a dataset acquired in the High Arctic, using the same UV-visible spectrometer as in this study is presented by Melo et al. (2004).

In brief, since the scattering geometry changes with SZA, a time series of slant column measurements contains information on the vertical distribution of NO$_2$ throughout the atmosphere. The NO$_2$ vertical distribution is then retrieved from the set of NO$_2$ slant columns measured over a range of SZAs during twilight using the optimal estimation method based on the algorithms for solving atmospheric inversion problems developed by Rodgers (1976, 1990, 2000). The linear approach is adopted since NO$_2$ is optically thin and so the forward model for zenith-sky measurements is essentially linear. The optimal estimation equations are solved sequentially to avoid matrix inversions. Essentially, optimal estimation minimizes the difference between the measurement and the calculated slant column values to determine the optimum solution profile. Additionally, it includes a formal treatment of the errors. As shown by Preston and co-workers, for zenith-sky measurements, the vertical resolution of the retrieved NO$_2$ profile varies from 5 to 7 km through the altitude range where the method is valid, which is approximately 10 to 35 km.

A forward model is used to calculate the NO$_2$ slant column for a given NO$_x$ (NO+NO$_2$) profile. This approach has the advantage of NO$_x$ being relatively constant with time during twilight. NO$_2$ profiles can then be derived from the retrieved NO$_x$ profile using the output of the photochemical model. The model incorporates scattering (including multiple scattering) by molecules and aerosols, absorption by O$_3$ and NO$_2$, and refraction. It consists of a stacked box model (Fish et al., 1997), and a radiative-transfer model, as described in Preston et al. (1998). The box model is initialized using a two-dimensional model interpolated to the appropriate latitude and time of year. The O$_3$ concentration, pressure and temperature profiles are taken from the ozonesonde data acquired during the MANTRA campaign for the days of interest. The a priori NO$_2$ profile used in the retrieval is calculated using the box model for each condition: sunrise and sunset.

The slant column measurement errors are quantified using an approximation described in Preston (1995). First, the differential optical depth due to all absorbers except NO$_2$ is calculated using the fitted amounts of these absorbers. This value is then subtracted from the total measured differential optical depth to give the measured optical depth of NO$_2$. Then, the measured optical depth of NO$_2$ is linearly regressed onto the NO$_2$ absorption cross-section. The slope of the linear regression is the slant column amount of NO$_2$ and the variance of the slope represents the slant column measurement error variance. This approach should be adopted only if the measurement errors are uncorrelated. However, we adopt it here even knowing that the errors in the slant column densities are dominated by systematic and not random error.

The assumption of the error in the a priori profile is also important in optimal estimation. If too low an error in the a priori state is assumed, it will result in a retrieval biased towards the a priori profile with less weight given to the information from the measurement. On the other hand, too loose a constraint, due to the assumption of a larger error in the a priori profile, results in the measurement being over-fitted and noise being interpreted as data. In this work we define the error in the a priori state at 50%. Note that both the measurement and a priori state error covariance matrices are assumed to be diagonal.

When zenith-sky spectra are analysed using DOAS, the quantity retrieved is the differential slant column density of the absorber. Since the observed spectrum for a given SZA is ratioed to the reference spectrum, in order to calculate the absolute slant column, the amount of NO$_2$ in the reference spectrum must be added to the retrieved slant column amount. A detailed discussion of the process used to determine the amount of NO$_2$ in the reference spectrum is given in Melo et al. (2004). In brief, the reference column density (*RCD*) for NO$_2$ is calculated as the mean slope of the Langley plots (i.e., the plot of differential NO$_2$ slant columns measured at SZAs from 80° to 85° on the same day against the corresponding NO$_2$ air mass factors, hereinafter referred to as *AMF*s) separately for sunrise and sunset. The *AMF*s are calculated using the radiative transfer model of McLinden et al. (2002) which simulates the transfer of radiation through the atmosphere and associated photon path lengths through a range of solar zenith angles. The *RCD* value used here is $0.78 \times 10^{16}$ molecules cm$^{-2}$. The absolute slant column densities are then the quantity used in the profile retrieval.

The determination of the amount of NO$_2$ in the reference spectrum can be somewhat arbitrary and may influence the retrieved profile. Melo et al. (2004) show that, for profiles retrieved using measurements taken in the Arctic, small differences in the assumed reference amount of NO$_2$ may lead to significant changes in the shape of the retrieved NO$_2$ profile. However, for the mid-latitude measurements analysed here, we observed that the shape of the profile around the peak altitude range is not affected by varying the reference amount of NO$_2$ by as much as 20%.

## 4 Results

The retrieval method described above is applied to all days for which we have ground-based observations, i.e., from 18 to 25 August 1998. Figure 1 shows the fitted and measured NO$_2$ absolute slant column densities as a function of SZA for 24 August. As can be seen, there is good agreement between the fitted and measured values for both sunrise and sunset, with a maximum difference of 13% at 80° SZA for sunset. Although not shown here, good agreement is also obtained for all the other days analysed.
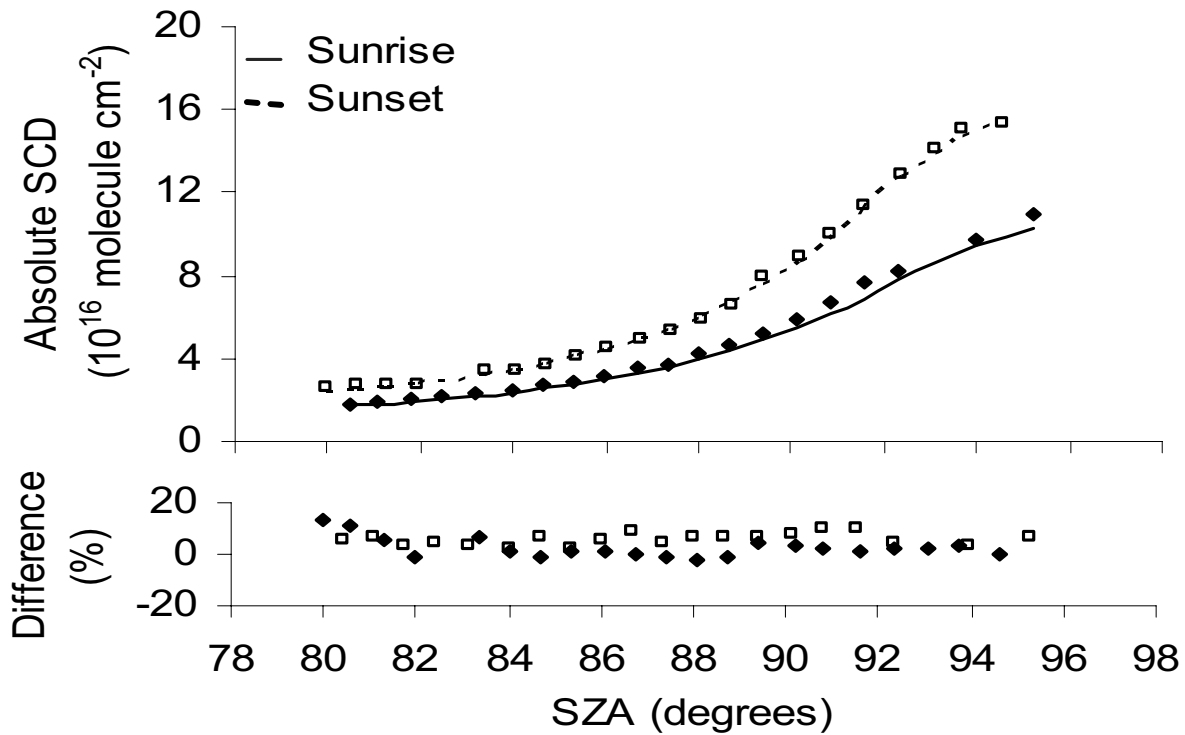
Fig. 1    The NO$_2$ slant columns measured with the ground-based UV-visible spectrometer on 24 August 1998 (symbols) and the fitted values (line). Lower plot: the percentage difference for ((measured-fitted)/measured), sunrise (diamonds) and sunset (squares).
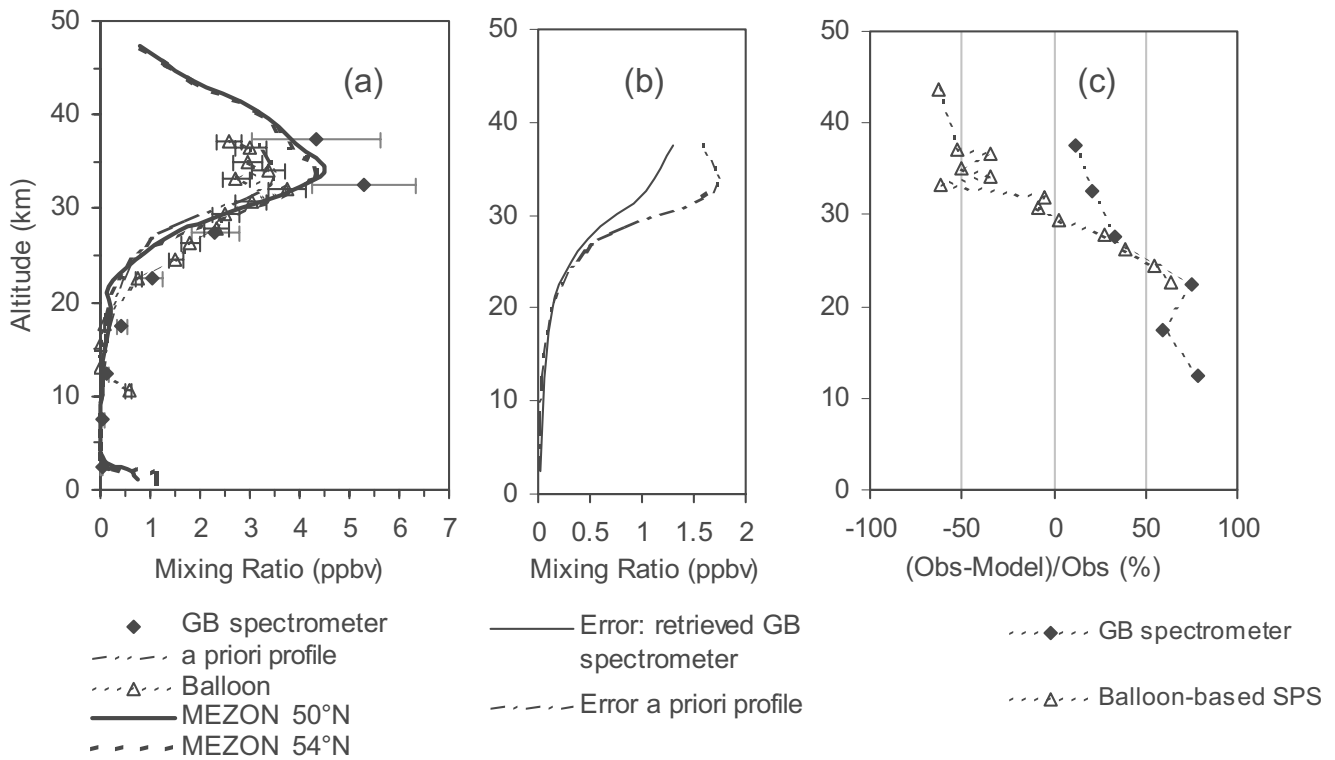


Fig. 2    (a) NO$_2$ vertical profile retrieved from the ground-based observations made at sunrise (90° SZA) on 24 August. Also shown are the coincident balloon-borne SPS profile and the MEZON model output for the same longitude and time, and the two closest latitudes (50°N and 54°N), and the a priori profile used for the ground-based retrieval. (b) The assumed error in the a priori NO$_2$ profile compared with the error in the retrieved NO$_2$ profile for sunrise. (c) Percentage difference model and observation: diamonds represent the ratio of ground-based retrieved NO$_2$ mixing ratio and the model for 50°N latitude; the open triangles represent the ratio between the balloon NO$_2$ measurements and the model also for 50°N latitude.

The retrieval algorithm produces NO$_2$ profiles in units of number density (molecules cm$^{-3}$). In order to compare them with the balloon-based measurements and later with the model, these NO$_2$ concentrations are converted to volume mixing ratio using the respective air density profiles measured by the sondes.

The NO$_2$ mixing ratio profile retrieved for sunrise on 24 August is shown in Fig. 2a, together with the co-located and coincident NO$_2$ profile measured with the balloon-borne SPS. This ground-based profile agrees with the balloon profile within the error bars for altitudes below the peak. Around the peak altitude, at 32.5 ± 5.0 km, the two profiles differ by about 30% with the ground-based maximum value (5.3 ± 1.0 ppbv) being larger than that measured from the balloon (3.7 ± 0.4 ppbv).

Our simulations using a smaller reference amount for this day show that even using zero as the reference amount, the upper part of the profile would not follow the balloon measurements. We observed that changes in the reference amount significantly affect only the bottom part of the retreived ground-based profile. Therefore we do not believe that the discrepancy among the ground-based retrieved and the balloon profile could be caused by the adoption of a too high value for the reference amount. As discussed in Rodgers and Connor (2003), intercomparison of measurements made by different remote sounding instruments requires that allowance be made for differing characteristics of the observing systems, particularly their averaging kernels and error covariances. Rodgers and Connor propose a method for carrying out such a comparison. The method is applied here by smoothing the profile retrieved with higher vertical resolution (the balloon-based profile, $X_{balloon}$) with the averaging kernels, $A$, and the a priori state for the ground-based profile, $Xa$. The smoothed profile, $X_{smoothed}$, is then:

$$X_{smoothed} = Xa + A(X_{balloon} - Xa) \qquad (1)$$

The balloon-based profile smoothed by the ground-based retrieval parameters and the ground-based profile are shown in Fig. 3. As can be seen from this figure, applying the smoothing method brings the profiles measured by different instruments closer together.

A caveat of the comparison between the ground-based and the balloon-borne profiles is that both measurements are based on the molecular absorption of sunlight in the UV-visible spectral region. However, the two instruments have different viewing geometry (zenith sky versus solar occultation) and the profiles were retrieved using different algorithms. Therefore, the good agreement between the two measured profiles in Figs 2 and 3 gives us confidence in the retrieval method adopted for the ground-based observations.

One of the difficulties in any retrieval technique is to assess the extent to which the measurements contribute to the retrieved values. The a priori profile used in the retrieval of NO$_2$ for sunrise on 24 August is shown, along with the retrieved profile, in Fig, 2a. As can be seen, the two profiles

are significantly different, indicating that we are not just getting the a priori profile back when doing the retrieval. Figure 2b compares the error assumed in the a priori profile (50%) with the retrieved error. The errors in the a priori and the retrieved profiles are the square root of the diagonal elements of the a priori and retrieved error covariance matrices, respectively. As can be seen from Fig. 2b, the error in the retrieved profile is smaller than the assumed error in the a priori profile at all altitudes above about 15 km, once more suggesting that the measurements have indeed contributed to the retrieved NO$_2$ profile.

Another way to address the issue of the extent to which the retrieved profile depends on the a priori profile is by looking at the averaging kernel matrix which is the product of the contribution function and the weighting function matrices. The averaging kernels indicate how the retrieval smoothes the true profile. Figure 4 shows the averaging kernels calculated for the retrieval using the ground-measurements taken at sunrise on 24 August. As can be seen from the figure, the averaging kernels for altitudes from 17.5 to 32.5 km have distinctive peaks, given the altitude resolution of the model, and peak at the altitude to which they correspond, indicating a larger contribution from the measurements at that altitude. For altitudes below 17 km and above 32 km, the averaging kernels are very broad and do not peak at their corresponding altitudes; therefore, the retrieved profiles at the top and the very bottom levels have a larger dependence on the a priori profile.

We have also carried out experiments using a model NO$_2$ profile converted to slant column density to which we applied a 15% random error. This experiment shows that we retrieve the NO$_2$ vertical profile we start with. A more detailed analysis in this direction is in process and will be presented in another publication.

Figure 5 (top panel) shows the retrieved NO$_2$ mixing ratios as a function of altitude and day of the year for both sunrise and sunset. It is important to emphasize that the plots presented in Fig. 5 are intended to facilitate visualization of day-to-day variability in the twilight NO$_2$ profiles. Note that each plot is built using only one retrieved profile a day (for each condition: sunrise and sunset taken as 90° SZA). From this figure we can see that the NO$_2$ mixing ratio consistently peaks at an altitude of approximately 32 km for all the days although the shape of the profiles varies from day to day. We also observe that broader profiles are associated with larger NO$_2$ amounts at the peak altitude.

The observed day-to-day variability in NO$_2$ mixing ratio as a function of altitude is quantified in Fig. 6 where the average retrieved mixing ratio profile over the duration of the campaign is shown together with the maximum and minimum values obtained for each altitude. Larger variability (to the average value), of the order of 35%, is observed around the mixing ratio peak altitude. The observed NO$_2$ mixing ratio day-to-day variability at the peak altitude is discussed later in this paper when comparing our results with the MEZON model output.
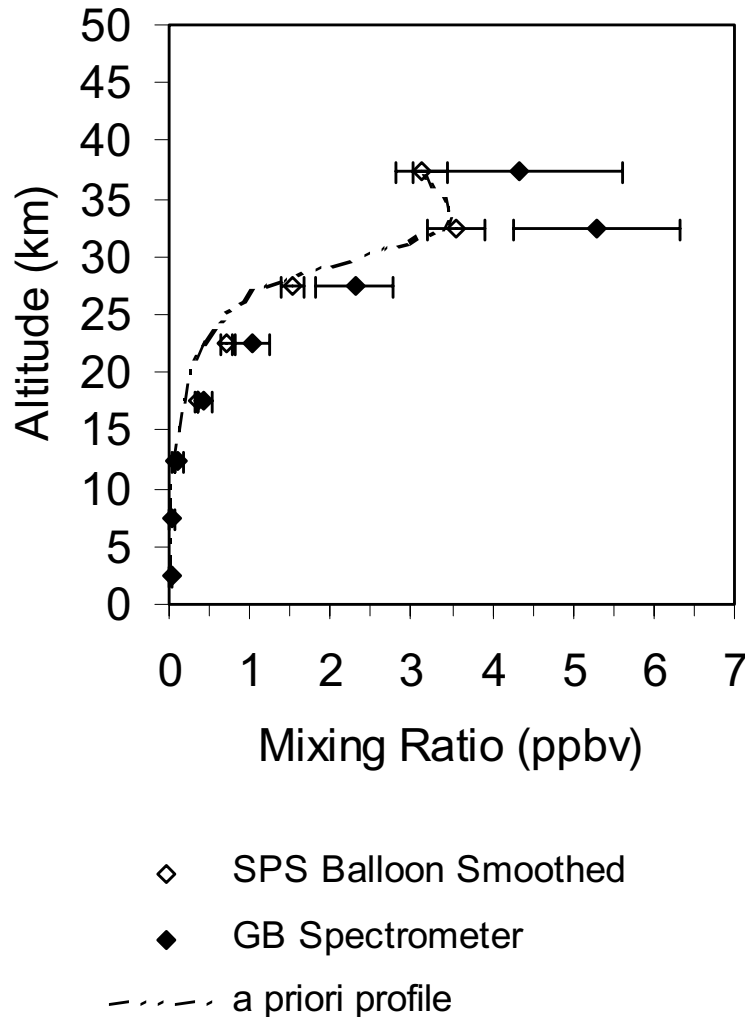
Fig. 3 NO$_2$ vertical profile retrieved from the ground-based measurements compared with the balloon-borne SPS profile smoothed to the resolution of the ground-based retrieved profile using the ground-based retrieved averaging kernels (see text). Also shown is the a priori for the ground-based retrieval.

One interesting aspect is the conversion of measured slant column densities to vertical column densities. When zenith-sky spectra are analysed using the DOAS retrieval procedure, the quantity retrieved is the slant column density, SCD, of the absorber as a function of the solar zenith angle, θ. However, the desired quantity is usually the vertical column density, VCD. The conversion of slant column density into vertical column density can be made through the assumption of an appropriate AMF using:

$$VCD(\theta) = (SCD(\theta) + RCD)/AMF(\theta), \qquad (2)$$

where RCD, the reference column density, represents the amount of absorber in the reference spectrum estimated from the Langley plots as discussed previously.

Although appropriate values for the AMF can be calculated using a radiative transfer model, these results are sensitive to the assumed vertical profiles of the absorber of interest.

The choice of the NO$_2$ profile to be used in the radiative transfer model can be particularly difficult due to the limited number of observations and the diurnal variation in NO$_2$ amount (Bassford et al., 2001). Often a modelled NO$_2$ profile or one measured under different conditions becomes the only available choice. Therefore, by retrieving the NO$_2$ mixing ratio profile directly from the measured SCD values, as we do here, the NO$_2$ vertical column density can be obtained directly by integrating each retrieved profile over altitude.

In Fig. 7a we compare the NO$_2$ vertical column densities for twilight (SZA = 90°) obtained by Bassford et al. (this issue) (who calculated the AMF) with the values obtained from the integration of the altitude profiles retrieved here in units of number density (molecules cm$^{-3}$). Observe that Bassford and co-workers adopted one value of AMF at 90° SZA for the entire campaign (AMF = 18.92), as is usually done. As can be seen from this figure, the values obtained for the vertical column using the retrieved NO$_2$ profiles are higher than those obtained using the calculated AMF. The AMF
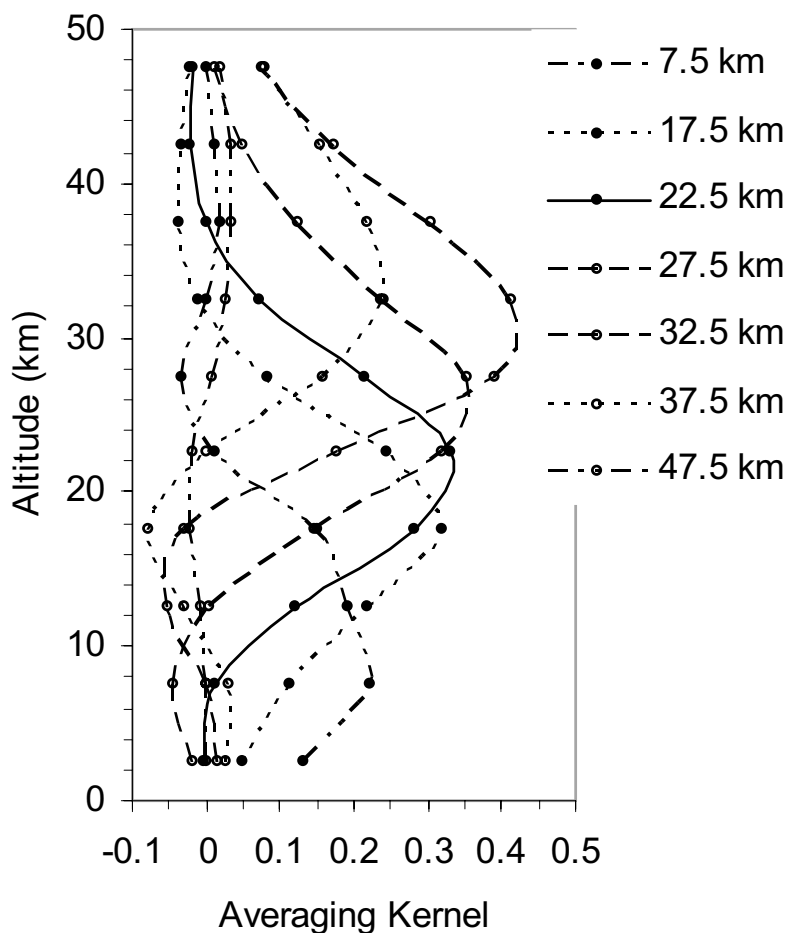
Fig. 4    Averaging kernels calculated for the sunrise retrieval using ground-based measurements taken on 24 August. Each averaging kernel corresponds to a different profile altitude (see legend).

value used by Bassford et al. (this issue) was calculated assuming a Gaussian NO$_2$ profile Full Width at Half Maximum intensity (FWHM=14 km) peaking at 34 km (10.7 ppbv) in the radiative transfer model of McLinden et al. (2002). This represents a much larger NO$_2$ peak maximum than that retrieved here, thus explaining why the *AMF* differs. The difference between the *AMF* values at 90° SZA obtained from the two methods is shown in Fig. 7b for both sunrise and sunset. As can be seen from this figure, this difference (which can be as large as 30% of the values calculated by Bassford et al. (this issue)) varies from day to day suggesting that an appropriate *AMF* should be calculated for each day of observation, and for sunset and sunrise. As shown in Fig. 5, we observed that the NO$_2$ profile indeed has a day-to-day variation, therefore the *AMF* calculations should ideally account for this, although this can be difficult to do in practice (see Bassford et al. (2001) for a discussion of *AMF* calculations). This clearly indicates that inter-instrument comparisons for NO$_2$ DOAS measurements, as well as long-term trend analysis, should indeed be conducted using measured slant column densities instead of the derived vertical column densities.

## 5 Comparison with a chemical transport model

Retrieved trace gas profiles provide an opportunity to test three-dimensional chemical transport models. The MANTRA 1998 balloon campaign offers a good opportunity for such comparison since the balloon flight took place in August, during the summer turnaround of the stratospheric zonal winds (a change in sign of the zonal wind velocity – see Wunch et al. (this issue)) and the stratospheric conditions are then as close as possible to photochemical equilibrium. In this paper we compare the retrieved NO$_2$ profiles with the output of the MEZON global chemistry-transport model.

MEZON is described in detail by Rozanov et al. (1999), Rozanov and Schlesinger (2001), and Egorova et al. (2003). It has a horizontal resolution of 4° in latitude and 5° in longitude. In the vertical direction, the model spans the atmosphere from the ground to 1 hPa. MEZON is driven by wind and temperature fields provided by the UK Met Office (UKMO) assimilation system (Swinbank and O'Neill, 1994). The photochemical part of the model calculates the distribution of forty-five chemical species that are determined by 118 gas-phase, 33 photolysis, and 16 heterogeneous reactions. The chemical solver utilizes a pure
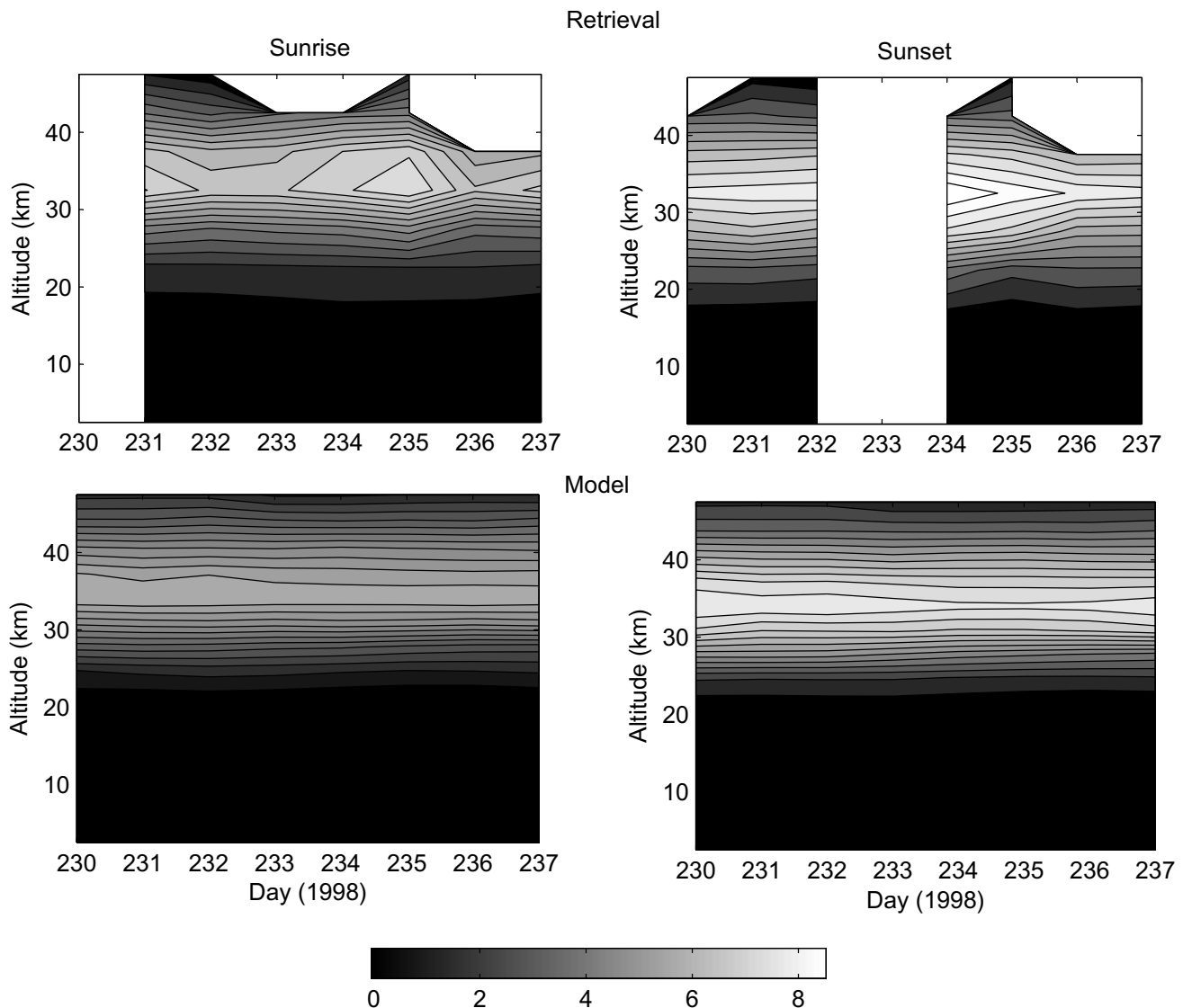
Retrieval



Fig. 5   NO$_2$ mixing ratio at 90° SZA as a function of altitude and day of the year for the MANTRA 1998 campaign at sunrise (left) and sunset (right). The two upper plots refer to the retrieved ground-based quantities while the two lower plots show the MEZON model output for sunrise (left) and sunset (right). The gap in the retrieved sunset results is due to lack of measurements caused by instrumental problems.

implicit iterative Newton-Raphson scheme (Rozanov et al., 1999). The reaction coefficients are taken from DeMore (1997) and Sander (2000). Photolysis rates are calculated at every step using the look-up-table approach of Rozanov et al. (1999) and the current values of the O$_3$ mixing ratio and spectral solar flux. The hybrid scheme of Zubov et al. (1999) is used for advective transport of species. The model time step is two hours. Polar stratospheric cloud (PSC) properties are calculated using a diagnostic thermodynamic scheme (Hanson and Maursberger, 1998; Chipperfield et al., 1993), which describes the condensation, sedimentation and evaporation of PSC particles in a simplified manner. Coefficients of the heterogeneous reactions on/in stratospheric aerosol and PSC particles have been adopted from Hanson et al. (1994) and DeMore (1997), respectively.

The initial conditions for the trace-gas concentrations have been taken from the Upper Atmosphere Research Satellite (UARS) data for September 1992. The ground-level monthly concentrations of CO$_2$, CH$_4$, N$_2$O, CFC-11, CFC-12, CH$_3$CCl$_3$, CCl$_4$, CH$_3$Cl, CHCl$_3$ and CCl$_2$FCClF$_2$ for each of the simulated years were taken from the National Oceanic and Atmospheric Administration/Climate Modeling and Diagnostic Laboratory (NOAA/CMDL) database, separately for the northern and southern hemispheres (Egorova et al., 2001). The surface fluxes of NO$_x$ and CO were acquired from Muller and Brasseur (1995). The same database was used to prescribe the lightning source of NO$_x$. With this model we have carried out an eight-year run from September 1992 to September 2000. Then, starting from June 1998, we performed
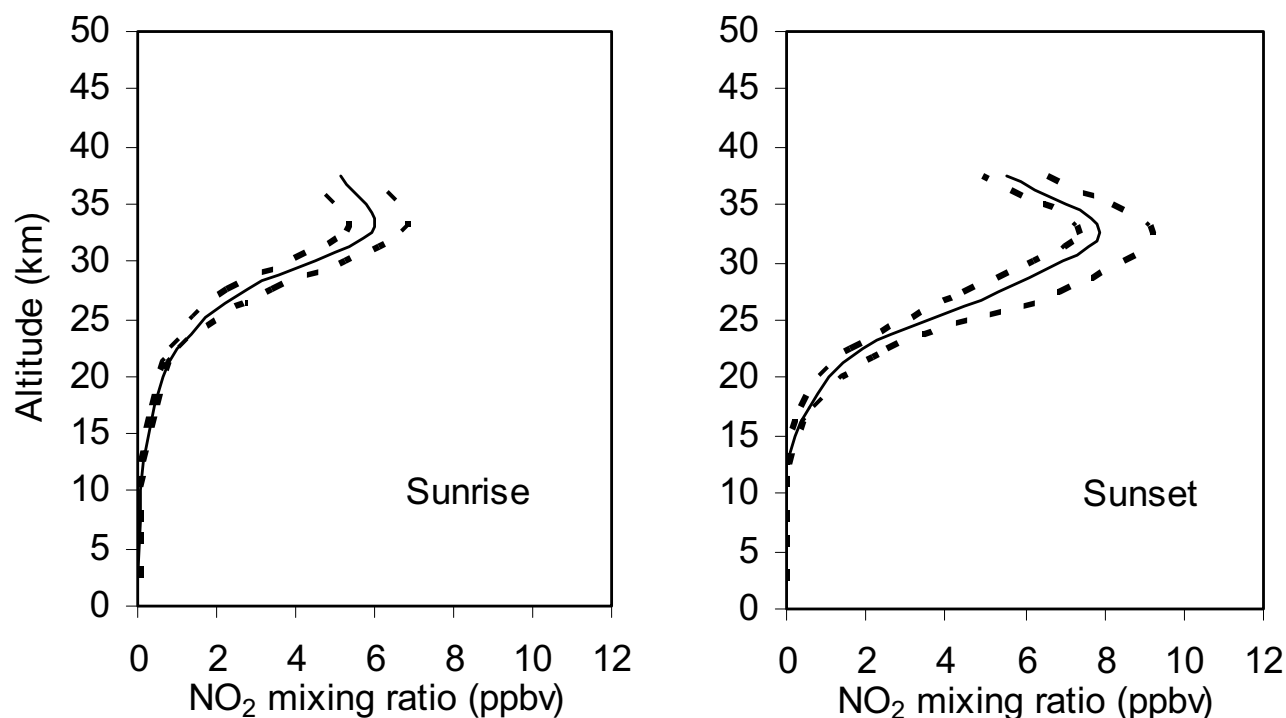
Fig. 6    The retrieved NO₂ mixing ratio as a function of altitude at 90° SZA for sunset and sunrise. The solid lines represent the average profile for the whole campaign (seven days sunset and seven days sunrise) while the dashed lines represent the maximum and the minimum values retrieved at each altitude.

a three-month run with a twenty-minute time step to produce the NO₂ profiles.

The output of MEZON for sunrise on 24 August 1998 for 50° and 54°N, and 108°W, is shown in Fig. 2a, together with the SPS profile and the profile retrieved from the ground-based observations. The model results for the two latitudes are quite similar, with the maximum mixing ratio of 4.53 ppbv at 34-km altitude for the 50°N latitude profile, and the maximum mixing ratio of 4.34 ppbv also at 34-km altitude for the 54°N latitude profile. As can be seen from the figure, those values agree with the observed values within the measurement error bars. The retrieved ground-based profile has a maximum in mixing ratio 2 km lower than the model prediction. Since the altitude resolution of the retrieved profiles at those altitudes is estimated to be around 5 km, the agreement with the model results for the altitude of the maximum mixing ratio can be considered reasonable. However, the model substantially underestimates NO₂ from 20- to 30-km altitude (30% at around 30-km altitude and 45% around 20-km altitude). Such aspects can be seen more clearly in Fig. 2c where the difference between the model and the measurements is shown, as a percentage of the measurements, as a function of altitude.

Figure 5 (bottom panels) shows MEZON output for 18 August (day 230) to 25 August (day 237) for sunrise and sunset. It can be seen that the modelled mixing ratio is again at a maximum at about 34 km for all the days analysed here. From Fig. 5 we can see that the day-to-day variability in the NO₂ mixing ratio maximum is more pronounced in the observations than in the model results. The variability in the model does not exceed 2% for the

days analysed. Changes in stratospheric NO₂ concentrations at mid-latitudes over a period of days were first shown by Noxon (1979), who attributed such variability to quasi-horizontal transport on a global scale. Large day-to-day variability has also been reported in ground-based BrO measurements at mid-latitudes by Fish et al. (1995). Using a one-dimensional model, Fish et al. (1995) investigated several possibilities including vertical air motion induced by changes in tropopause height, latitudinal transport, changes in stratospheric temperature and tropospheric changes. Although not conclusive, the investigations of Fish et al. (1995) suggest that the meridional advection of air and changes in stratospheric temperature would be the most relevant processes in inducing the observed day-to-day variability in BrO. The day-to-day variability in NO₂ reported here, as well as possible year-to-year variability are being investigated using results from all four MANTRA campaigns (1998, 2000, 2002, and 2004) along with different atmospheric models and are the subject of a future paper.

**6 Summary**

We have reported here on the use of a retrieval technique to recover NO₂ mixing ratio profiles from ground-based slant column measurements. The observations were made with a UV-visible zenith-sky spectrometer operated on the ground from 18 to 25 August 1998 during the MANTRA balloon campaign at Vanscoy, Saskatchewan. The NO₂ profile retrieved from the ground-based observations was compared with the co-located and simultaneous profile measured by a balloon-borne UV-visible SPS during sunrise on 24 August
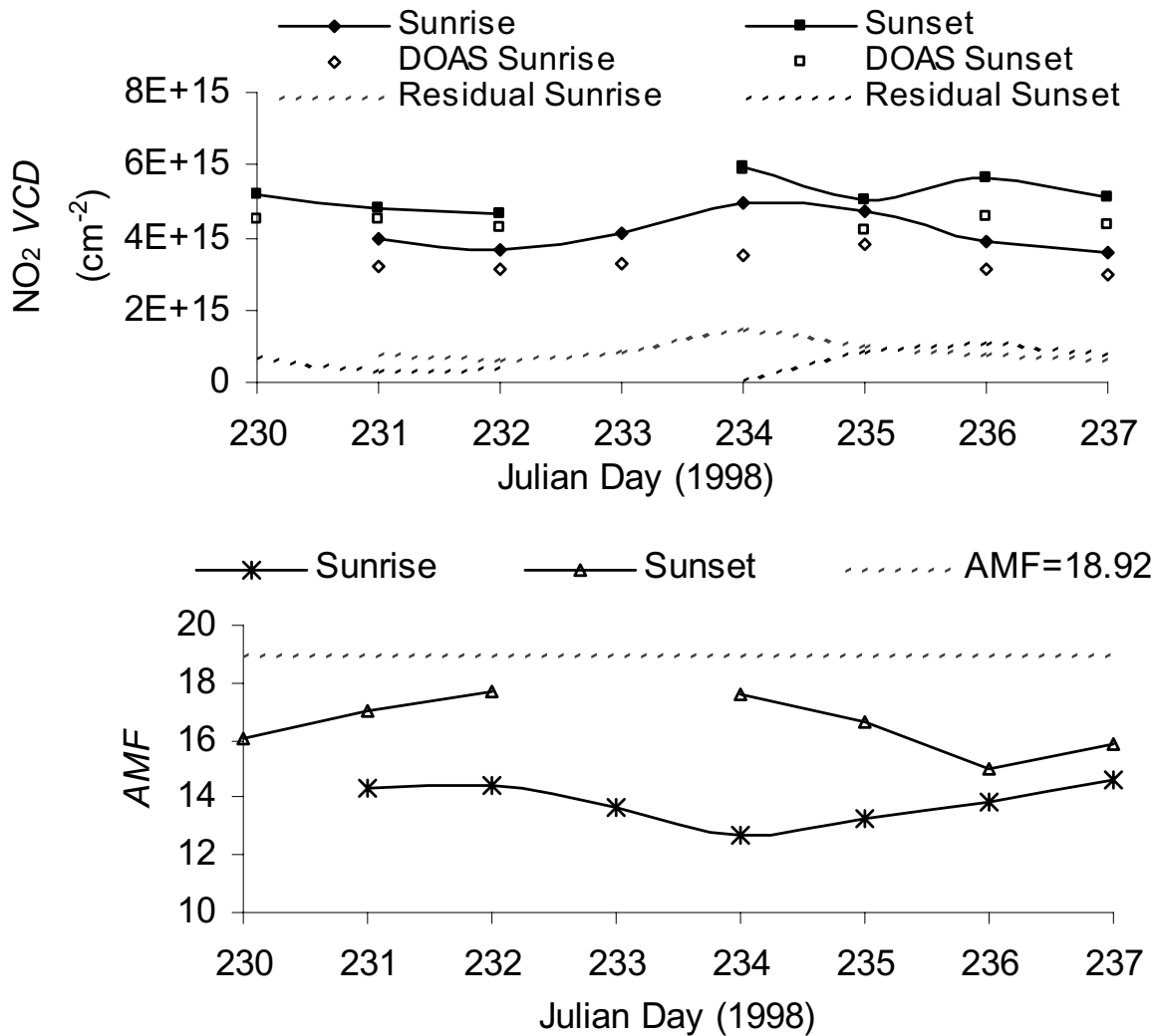
Fig. 7 (a) NO$_2$ vertical column density values from DOAS measurements at SZA = 90° (Bassford et al., this issue) adopting a calculated *AMF*, compared with the values obtained from the integration of the vertical profiles retrieved here. (b) The *AMF* value used by Bassford et al. (this issue) compared with the *AMF* values obtained here.

and with the output of the MEZON 3-D stratospheric chemical transport model. Good agreement is observed between the two retrieved NO$_2$ profiles for altitudes below the peak mixing ratio. At the peak and above, the ground-based retrieval overestimates the NO$_2$ mixing ratio relative to the balloon-borne measurement. Interestingly the MEZON model underestimates both observations at lower altitudes, while producing values between the two measurements for altitudes around the peak mixing ratio. Our results indicate that the ground-based retrieval method discussed here produces reliable results for the NO$_2$ mixing ratio at the peak altitude and below it. However, the absolute values for the mixing ratio should be used with caution. Further work to investigate the reliablity and sensitivity of NO$_2$ profile retrievals using ground-based UV-visible spectroscopy is ongoing.

**Note Added in Proof**

After acceptance of the paper, revised absorption cross-sections of NO$_2$ became available. Figures 2 and 3 which were originally based on GOME cross-sections have been modified to make use of the more recent van Daele cross-sections.

# References

BASSFORD, M. R.; C. A. MCLINDEN and K. STRONG. 2001. Zenith-sky observations of stratospheric gases: the sensitivity of air mass factors to geophysical parameters and the influence of tropospheric clouds. *J. Quant. Spectrosc. Radiat. Transfer*, **68**: 657–677.

——; K. STRONG, C. A. MCLINDEN and C. T. MCELROY. 2005. Ground-based measurements of ozone and NO$_2$ during MANTRA 1998 using a zenith-sky spectrometer. ATMOSPHERE-OCEAN, **43**: 325–338.

BREWER, A. W.; C. T. MCELROY and J. B. KERR. 1973. Nitrogen dioxide concentration in the atmosphere. *Nature*, **246**: 129–133.

BURROWS, J. P.; A. DERN, B. DETERS, S. HIMMEIMANN, A. RICHTER, S. VOIGHT and J. ORPHAL. 1998. Atmospheric remote-sensing reference data from GOME. Part 2: temperature-dependent absorption cross-sections of NO$_2$ in the 231–794 nm range. *J. Quant. Spectrosc. Radiat. Transfer*, **60**: 1025–1031.

CHANCE, K. V. and R. J. D. SPURR. 1997. Ring effect studies: Rayleigh scattering, including molecular parameters for rotational Raman scattering, and the Fraunhofer spectrum. *Appl. Opt.* **36**: 5224–5230.

CHIPPERFIELD, M.; D. CARIOLLE, P. SIMON, R. RAMAROSON and D. LARRY. 1993. A three-dimensional modeling study of trace species in the Arctic lower stratosphere during winter 1989–1990. *J. Geophys. Res.* **98**: 7199–7218.

CRUTZEN, P. J. 1970. The influence of nitrogen oxides on the atmospheric ozone content. *Q. J. R. Meteorol. Soc.* **96**: 320–325.

DEMORE, W. B.; C. J. HOWARD, S.P. SANDER, A. R. RAVISHANKARA, D. M. GOLDEN, C. E. KOLB, R. F. HAMPSON, M. J. MOLINA and M. J. KURYLO. 1997. Chemical kinetics and photochemical data for use in stratospheric modeling, Evaluation No. 12, NASA Jet Propulsion Laboratory, JPL Publication 97–4, 278 pp.

EGOROVA, T. A.; R. E. V. ROZANOV, M. E. SCHLESINGER, N. G. ANDRONOVA, S. L. MALYSHEV, I. L. KAROL and V. A. ZUBOV. 2001. Assesment of the effect of the Montreal Protocol on atmospheric ozone. *Geophys. Res. Lett.* **22**: 2389–2392.

——; E. ROZANOV, V. ZUBOV and I. KAROL. 2003. Model for investigating ozone trends (MEZON). *Atmos. Oceanic Phys.* **39**: 277–292.

FAHEY, D. W.; R. S. GAO, K. A. CARSLAW, J. KETTLEBOROUGH, P. J. POPP, M. J. NORTHWAY, J. C. HOLECEK, S. C. CICIORA, R. J. MCLAUGHLIN, T. L. THOMPSON, R. H. WINKLER, D. G. BAUMGARDER, B. GANDRUD, P. O. WENNBERG, S. DHANIYALA, K. MCKINNEY, T. PETER, R. J. SALAWITCH, H. JOST, J. C. WILSON, R. L. HERMAN, A. KLEINBÖHL AND M. VON KÖNIG. 2001. The detection of large HNO$_3$ particles in the winter Arctic stratosphere. *Science*, **291**: 1026–1031.

FIOLETOV, V. E. and T. G. SHEPHERD. 2003. Seasonal persistence of midlatitude total ozone anomalies. *Geophys. Res. Lett.* **30**: 1417.

FISH, D. J.; T. L. JONES and R. K. STRONG. 1995. Midlatitude observations of the diurnal variation of stratospheric BrO. *J. Geophys. Res.* **100**: 18,863–18,871.

——; S. R. ALIWELL and R. L. JONES. 1997. Mid-latitude observations of the seasonal variation of BrO. Interpretation and modelling study. *Geophys. Res. Lett.* **24**: 1199–1202.

GARCIA, R. R. and S. SOLOMON. 1994. A new numerical model of the middle atmosphere, 2, ozone and related species. *J. Geophys. Res.* **99**: 12937–12953.

GRAINGER, J. F. and J. F. RING. 1962. Anomalous Fraunhofer line profiles. *Nature*, **193**: 762.

GREENBLATT, G. D.; J. J. ORLANDO, J. B. BURKHOLDER and A. R. RAVISHANKARA. 1990. Absorption measurements of oxygen between 330 and 1140 nm. *J. Geophys. Res.* **95**: 18,577–18,582.

HANSON, D.; A. RAVISHANKARA and S. SOLOMON. 1994. Heterogeneous reactions in sulfuric acid aerosols: A framework for model calculations. *J. Geophys. Res.* **99**: 3615–3629.

—— and K. MAURSBERGER. 1998. Laboratory studies of the nitric acid trihydrate: Implications for the south polar stratosphere. *Geophys. Res. Lett.* **15**: 855–858.

MCAFEE, J. R.; K. S. GAGE and R. G. STRAUCH. 1994. Examples of vertical velocity comparison from collocated VHF and UHF profilers. *Radio Sci.* **29**: 879–880.

MCELROY, C. T. 1995. A spectroradiometer for the measurement of direct and scattered solar irradiance from on-board the NASA ER-2 high altitude research aircraft. *Geophys. Res. Lett.* **22**: 1361–1364.

MCKENZIE, R. L.; P. V. JOHNSTON, C. T. MCELROY. J. B. KERR and S. SOLOMON. 1991. Altitude distribution of stratospheric constituents from ground-based measurements at twilight. *J. Geophys. Res.* **96**: 15499–15511.

MCLINDEN, C. A.; J. C. MCCONNELL, E. GRIFFIOEN and C. T. MCELROY. 2002. A vector radiative-transfer model for the Odin/OSIRIS project. *Can. J. Phys.* **80**: 375–393.

MELO, S. M. L.; E. FARAHANI, K. STRONG, M. R. BASSFORD, K. E. PRESTON and C. A. MCLINDEN. 2004. NO$_2$ vertical profiles retrieved from ground-based measurements during spring 1999 in the Canadian Arctic. *Adv. Space Res.* **34**: 786–792.

MULLER, J. F. and G. P. BRASSEUR. 1995. IMAGES: A three-dimensional chemical transport model of the global troposphere. *J. Geophys. Res.* **100**: 16,445–16,490.

NOXON, J. F. 1975. Nitrogen dioxide in the stratosphere and troposphere measured by ground-based absorption spectroscopy. *Science*, **189**: 547–549.

——. 1979. Stratospheric NO$_2$ 2. Global behavior. *J. Geophys. Res.* **84**: 5067–5076.

OTTEN, C.; F. FERLEMANN, U. PLATT, T. WAGNER and K. PFEILSTICKER. 1998. Ground-based DOAS UV/visible measurements at Kiruna (Sweden) during the SESAME winters 1993/94 and 1994/95. *J. Atmos. Chem.* **30**: 141–162.

PLATT, U. 1994. Differential optical absorption spectroscopy (DOAS). *Air Monitoring by Spectroscopic Techniques*. M. W. Sigrist (Ed.), Chemical Analysis Series, Vol. 127, John Wiley and Sons, Inc., New York, pp. 27–84.

PRESTON, K. E. 1995. The retrieval of NO$_2$ vertical profiles from ground-based twilight UV-Visible absorption measurements, Ph.D. Thesis, Pembroke College, University of Cambridge, 214 pp.

——; R. L. JONES and H. K. ROSCOE. 1997. Retrieval of NO$_2$ vertical profiles from ground-based UV-visible measurements: Method and validation. *J. Geophys. Res.* **102**: 19089–19097.

——; D. J. FISH, H. K. ROSCOE and R. L. JONES. 1998. Accurate derivation of total and stratospheric vertical columns of NO$_2$ from ground-based zenith-sky measurements. *J. Atmos. Chem.* **30**: 163–172.

RODGERS, C. D. 1976. Retrieval of atmospheric temperature and composition from remote measurements of thermal radiation. *Rev. Geophys. Sp. Phys.* **14**: 609–624.

——. 1990. Characterization and error analysis of profiles retrieved from remote sounding measurements. *J. Geophys. Res.* **95**: 5587–5595.

——. 2000. *Inverse methods for atmospheric sounding: Theory and practice*. World Scientific Inc., 256 pp.

—— and B. J. CONNOR. 2003. Intercomparison of remote sounding instruments. *J. Geophys. Res.* **108**: 4116–4130.

ROZANOV, E. V., V. A. ZUBOV, M. E. SCHLESINGER, F. YANG and N. G. ANDRONOVA. 1999. The UIUC 3-D stratospheric chemical transport model: Description and evaluation of the simulated source gases and ozone. *J. Geophys. Res.* **104**: 11,755–11,781.

—— and M. E. SCHLESINGER. 2001. The University of Illinois, Urbana-Chamapign three-dimensional stratospheric-tropospheric general circulation model with interactive ozone photochemistry: Fifteen-year control run climatology. *J. Geophys. Res.* **106**: 1–22.

SANDER, S. P. J. R. R. FRIEDL, W. B. DEMORE, D. M. GOLDEN, M. J. KURYLO, R. F. HAMPSON, R. E. HUIE, G. K. MOORTGAT, A. R. RAVISHANKARA, C. E. KOLB and M. J. MOLINA. 2000. Chemical kinetics and photochemical data for use in stratospheric modeling, NASA panel for data evaluation. JPL Publication 00-3, Jet Propulsion Laboratory Pasadena. Evaluation No.13.

SARKISSIAN, A. 1992. Observation depuis le sol des nuages et des poussières dans l'atmosphère. Applications à la stratosphère polaire et à l'atmosphère de Mars, Ph. D Thesis, Université de Paris.

SOLOMON, S.; A. L. SCHMELTEKOPF and R. W. SANDERS. 1987. On the interpretation of zenith sky absorption measurements. *J. Geophys. Res.* **92**: 8311–8319.

STRONG, K.; G. BAILAK, D. BARTON, M. R. BASSFORD, R. D. BLATHEIWICK, S. BROWN, D. CHARTRAND, J. DAVIES, J. R. DRUMMOND, P. F. FOGAL, E. FORSBERG, R. HALL, A. JOFRE, J. KAMINSKI, J. KOSTERS, C. LAURIN, J. C. MCCONNELL, C. T. MCELROY, C.A. MCLINDEN, S.M.L. MELO, K. MENZIES, C. MIDWINTER, F. J. MURCRAY, C. NOWLAN, R. J. OLSON, B. M. QUINE, Y. ROCHON, V. SAVASTIOUK, B. SOLHEIM, D. SOMMERFELDT, A. ULLBERG, S. WERCHOHLAD, H. WU and D. WUNCH. 2005. MANTRA - A balloon mission to study the odd-nitrogen budget of the stratosphere. ATMOSPHERE–OCEAN, **43**: 283–299.

SWINBANK, R. and A. O'NEILL. 1994. A stratosphere-troposphere data assimilation system. *Mon. Weather Rev.* **122**: 686–702.

WUNCH, D.; M. P. TINGLEY, T. G. SHEPHERD, J. R. DRUMMOND, G. W. K. MOORE and K. STRONG. 2005. Climatology and predictability of the late summer stratospheric zonal wind turnaround over Vanscoy, Saskatchewan. ATMOSPHERE–OCEAN, **43**: 301–313

ZUBOV, V. A.; E. V. ROZANOV and M. E. SCHLESINGER. 1999. Hybrid scheme for 3-dimentional advective transport. *Mon. Weather Rev.* **127**: 1335–1346.